HOSTED BY

ELSEVIER

Available online at www.sciencedirect.com

ScienceDirect

Journal of Radiation Research and Applied Sciences

journal homepage: http://www.elsevier.com/locate/jrras

Characterization of silver nanoparticles synthesized using *Urtica dioica* Linn. leaves and their synergistic effects with antibiotics

Kumari Jyoti, Mamta Baunthiyal, Ajeet Singh *

Department of Biotechnology, Govind Ballabh Pant Engineering College, Pauri Garhwal, Uttarakhand, 246194, India

ARTICLE INFO

Article history:
Received 26 July 2015
Accepted 7 October 2015
Available online 21 October 2015

Keywords:
Urtica dioica Linn.
AgNPs
TEM
Antibacterial synergy

ABSTRACT

In continuation of the efforts for synthesizing silver nanoparticles (AgNPs) by green chemistry route, here we report a facile bottom-up 'green' route for the synthesis of AgNPs using aqueous leaves extract of *Urtica dioica* (Linn.). The synthesized AgNPs were characterized by UV-vis spectroscopy, X-ray diffraction (XRD), Fourier transform-infrared spectroscopy (FTIR), Zeta-sizer and Zeta-potential, Scanning electron microscopy (SEM), Energy dispersive X-ray (EDX) spectroscopy, Transmission electron microscopy (TEM) and Selected area electron diffraction (SAED). The results obtained from various characterizations revealed that AgNPs were in the size range of 20–30 nm and crystallized in face-centered-cubic structure. The antibacterial activity against Gram-positive (*Bacillus cereus*, *Bacillus subtilis*, *Staphylococcus aureus* and *Staphylococcus epidermidis*) and Gram-negative (*Escherichia coli*, *Klebsiella pneumoniae*, *Serratia marcescens* and *Salmonella typhimurium*) bacterial pathogens was demonstrated by synthesized nanoparticles. Further, synergistic effects of AgNPs with various antibiotics were evaluated against above mentioned bacterial pathogens. The results showed that AgNPs in combination with antibiotics have better antibacterial effect as compared with AgNPs alone and hence can be used in the treatment of infectious diseases caused by bacteria. The maximum effect, with a 17.8 fold increase in inhibition zone, was observed for amoxicillin with AgNPs against *S. marcescens* proving the synergistic role of AgNPs. Therefore, it may be used to augment the activities of antibiotics.

1. Introduction

Currently, there have been stupendous efforts to develop clean, non toxic, reliable and eco-benign procedures for the synthesis and assembly of nanoparticles with desired sizes and morphologies to expand their biomedical applications. Nanobiotechnology dealing with metal nanoparticles has drawn increasing attention due to its cutting-edge nature and wide application range in almost every field of science and technology including biomedical sciences. Presently, metal nanoparticles are of much importance because of their catalytic activity, optical properties, electronic properties, antimicrobial activity and magnetic activity (Duran, Marcarto,

* *Corresponding author*. Tel.: +91 9997178236; fax: +91 1368228062.
E-mail address: ajeetsoniyal@gmail.com (A. Singh).
Peer review under responsibility of The Egyptian Society of Radiation Sciences and Applications.
http://dx.doi.org/10.1016/j.jrras.2015.10.002

DeSouza, Alves, & Esposito, 2007; Kowshik et al., 2003). In medicine, nanomaterials have been used in specific applications such as tissue engineered scaffolds and devices, drug delivery systems, cancer therapy and bioanalytical diagnostics and therapeutics (Namasivayam, Gnanendra, & Reepika, 2010; Mukherjee et al., 2014; Vlerken & Amiji, 2006). There are a large numbers of physical, chemical, biological and hybrid methods available to synthesize metal nanoparticles (Tiwari, Behari, & Sen, 2008). Generally, physical and chemical methods are nonecofriendly, toxic and low in yield. The nanoparticles synthesized from chemical methods are medically non applicable because of contamination from precursor chemicals (Mallick, Witcomb, & Scurell, 2004). Natural environment is a rich source of crude untreated extract from tissues of various plants having miscellaneous chemical compounds. Thus, secrets discovered from nature have led to the development of green chemistry approaches for the fabrication of nanostructured materials. The green routes for the fabrication of nanoparticles have added advantages like ecofriendliness, low cost, energy efficient and compatibility with pharmaceuticals over physical, chemical and microbial synthesis (Chandran, Chaudhary, Pasricha, Ahmed, & Sastry, 2006).

Over the past several years, synthesis of various nanoparticles such as palladium, selenium, platinum, gold and silver using algae, fungi, bacteria and plant extracts is already reported in literature (Dubey, Lahtinen, & Sillanpaa, 2010; Kasthuri, Kathiravan, & Rajendiran, 2009; Rati et al., 2011; Sunita, Veera, Tushar, Robert, & Sudarshan, 2011; Sheny, Philip, & Mathew, 2012; Torres et al., 2012). Plant extracts have enzymes (hydrogenases, reductases) and phytochemicals such as terpenoids, flavonoids, phenols and dihydric phenols (Jacob, Biswas, Mukherjee, & Kapoor, 2011; Jha, Prasad, Prasad, & Kulkarni, 2009; Raghunandan et al., 2010; Thakkar, Mhatre, & Parikh, 2010) and so on to act as reductants in the presence of metal salt for nanoparticles synthesis. *Urtica dioica* Linn. (stinging nettle) is a herbaceous perennial flowering plant of the *Urticaceae* family. This plant has been reported to possess antibacterial, antifungal, antiviral, antioxidative activity (Gulcin, Kufrevioglu, Oktay, & Buyukokuroglu, 2004). However till date, this plant has not been reported for the synthesis of AgNPs. In view of this background, this plant is chosen as a reducing and stabilization/capping agent for the synthesis of silver nanoparticles as well as their characterization and applications in therapeutics. Silver has been used in many traditional medicines of Ayurveda and Roman times, therefore attracted attention as antimicrobial agent (Ashokkumar, Ravi, Kathiravan, & Velmurugan, 2014). Silver nanoparticles were proved to be more efficient in their antimicrobial activities against bacteria, fungi, viruses, and other eukaryotic microorganisms (Saravanan, Vemu, & Barik, 2011; Edgar, Sofia, Sonia, & Correia, 2014). Many researchers support that use of metallic silver as well as silver nanoparticles can be exploited in the field of medicine, dental materials, textiles fabrics, water treatment etc., and possess low toxicity to human cells, low volatility and high thermal stability (Duran et al., 2007; Jeyaraj et al., 2013; Kumar, Govindaraju, Senthamilselvi, & Premkumar, 2013; Prakash, Gnanaprakasam, Emmanuel, Arokiyaraj, & Saravanan, 2013). Human pathogens mainly bacteria have developed resistance against most of the antibiotics resulting their decreasing efficacy. To find out the solution of this problem is a challenge in medical science, therefore, we need to find environmentally benign biomaterial/bioresources in the synthesis of silver nanoparticles and their synergistic role with antibiotics. There are no reports concerning synthesis of AgNPs from *U. dioica* Linn., their antibacterial activity and synergistic effects with antibiotics against a wide group of pathogenic bacteria.

2. Materials and methods

2.1. Materials

2.1.1. Plant and chemicals

The leaves of *U. dioica* Linn. were collected from Govind Ballabh Pant Engineering College campus and the sample was authenticated by the taxonomist of Department of Botany, Hemwati Nandan Bahuguna Garhwal University (Central University) Srinagar, Uttarakhand. Silver nitrate ($AgNO_3$, 99%), Nutrient agar (NA), Antibiotic Disks, Mueller-Hinton Agar (MHA), Mueller-Hinton broth (MHB), H_2SO_4, copper acetate, ferric chloride, ninhydrin, HCl, Fehling's A and B solutions, iodine and potassium iodide were purchased from Sigma–Aldrich, Delhi. All the chemicals were of analytical reagent grade and were used without further purification. Milli-Q water was utilized in all the experiments.

2.1.2. Cultures

Standard cultures for antibacterial assays were procured from Microbial Type Culture Collection (MTCC), IMTECH, Chandigarh, India. These include Gram-positive (*Bacillus cereus* 4079, *Staphylococcus epidermidis* 3615, *Staphylococcus aureus* 740 and *Bacillus subtilis* 441) and Gram-negative (*Escherichia coli* 443, *Salmonella typhimurium* 98, *Klebsiella pneumoniae* 3384 and *Serratia marcescens* 97) bacterial pathogens.

2.2. Methods

2.2.1. Preparation of U. dioica *Linn. leaves extract*

20 g of finely cut leaves were thoroughly washed with running tap water and then with Milli-Q water to remove dirt and soil. The washed leaves were boiled in 100 ml Milli Q water for 15 min to get extract. The cooled extract was filtered through Whatman filter paper No. 1. The filterate was collected and stored at 4 °C till further use. This extract was used as reducing as well as stabilization/capping agent.

2.2.2. Phytosynthesis of AgNPs

Ag^+ ions were reduced by addition of 2.5 ml of *U. dioica* Linn. leaves extract to 47.5 ml of 10^{-3} M aqueous $AgNO_3$ solution in a 100 ml Erlenmeyer flask and kept for incubation at 40 °C for 60 min. The overall reaction process was carried out in dark to avoid unnecessary photochemical reactions. The color change of the $AgNO_3$ solution from colorless to dark brown was observed by naked eye and phyto-reduced sample component was confirmed by Ultraviolet-visible spectroscopy. The obtained AgNPs were purified through repeated centrifugation at 10,000 rpm for 20 min and dispersion of the pellet in Milli-Q

water to remove unbound particles and further used for characterization.

2.2.3. *Phytochemical screening*

The aqueous extract of *U. dioica* Linn. leaves and synthesised AgNPs were investigated for the presence of phytochemicals viz. carbohydrates, alkaloids, saponins, proteins, amino acids, phenol, diterpenes, tannins and phytosterols by following standard biochemical methods (Fransworth, 1996).

2.2.4. *Characterization of AgNPs*

Formation of AgNPs was confirmed by Ultraviolet-visible spectral analysis. The absorbance spectra were recorded using Ultraviolet-visible spectroscopy (UV-1800 Shimadzu UV spectrophotometer) at a wavelength of 300–700 nm. Fourier Transform Infrared Spectroscopy (FTIR) was performed on Thermo scientific™ Nicolet iS™50 FTIR Spectrometer to detect the possible functional groups in biomolecules present in the plant extract. The X-ray diffraction (XRD) measurement was performed on X-ray diffractometer (Panalytical Xpert-PRO 3050/60) operated at 30 kV and 100 mA and spectrum was recorded by CuKα radiation with wavelength of 1.5406 Å in the 2θ range of 20°–80°. The surface morphology and size of the AgNPs were examined using a Scanning electron microscope (SEM) and Energy dispersive X-ray (EDX) on NOVA-450 instrument and Transmission electron microscope (TEM), Selected area electron diffraction (SAED) measurements on Tecnai G2 20 S-TWIN instrument. The particle size distribution and surface charge of AgNPs were determined using particle size analyzer (Zetasizer nano ZS, Malvern Instruments Ltd., U.K.) at 25 °C with 90° detection angle.

2.2.5. *Antibacterial activity of AgNPs*

The antibacterial assays of the phytosynthesized AgNPs was assessed by using the Kirby–Bauer method (Cormican, Wilke, Barrett, Pfaller, & Jones, 1996) against human pathogenic Gram-positive (*B. cereus*, *S. epidermidis*, *S. aureus* and *B. subtilis*) and Gram-negative (*E. coli*, *S. typhimurium*, *K. pneumoniae* and *S. marcescens*) bacteria grown in Mueller-Hinton Agar medium at 37 °C for 24 h. Freshly cultured bacterial colonies of tested bacteria were taken and 100 µl of inoculum was spread on each Mueller-Hinton agar plates. Sterile Whatman filter paper disks (6 mm in diameter) were loaded with 0.05, 0.15, 0.25, 0.35 and 0.45mg/disk of synthesized AgNPs. The plant extract and $AgNO_3$ were used as control in each plate and incubated at 37 °C for 24 h. The plates were examined for presence of zones of inhibition, indicated by clear area around the discs. The diameters of inhibiton zones were measured and the mean value for each organism was recorded.

2.2.6. *Disk diffusion assay to evaluate synergistic effect*

The synergistic effects of phytosynthesized AgNPs with antibiotics against test strains on Mueller-Hinton Agar plates were studied using disk diffusion method. The standard antibiotic disks were purchased from Sigma Aldrich, Delhi. To determine the synergistic effects, each standard antibiotic disk was further impregnated with 10 µl of freshly prepared AgNPs. Mueller-Hinton Agar plates were inoculated with fresh inoculum of each culture and standard antibiotics disks with and without phytosynthesized AgNPs were placed and kept for incubation at 37 °C. After 24 h, the zones of inhibition were measured and the assays were performed in triplicate.

Table 1 – Phytochemical profile of *Urtica dioica* Linn. leaves and synthesized AgNPs.

Phytoconstituents	Screening	
	Plant extract	AgNPs
Carbohydrates	+	–
Alkaloids	+	–
Saponins	+	–
Proteins	+	+
Amino acid	+	–
Phenol	+	+
Diterpenes	+	+
Tannins	+	–
Phytosterols	+	+

3. Results and discussion

3.1. *Phytochemical screening*

The results of qualitative screening of phytochemicals in the extract of *U. dioica* Linn. leaves and AgNPs are shown in (Table 1). Phytochemical profile of *U. dioica* Linn. leaves revealed the presence of carbohydrates, alkaloids, saponins, proteins, amino acids, phenol, diterpenes, tannins and phytosterols. Synthesized AgNPs showed the presence of proteins, phenols, diterpenes and phytosterols which may be responsible for the efficient capping and stabilization of nanoparticles and this was further confirmed by FTIR spectrum.

3.2. *UV-Visible absorption studies*

The synthesis of the AgNPs in aqueous solution was monitored by recording the absorption spectra at a wavelength range of 300–700 nm (Fig. 1). It was observed that solution of silver nitrate turned dark brown on addition of leaves extract;

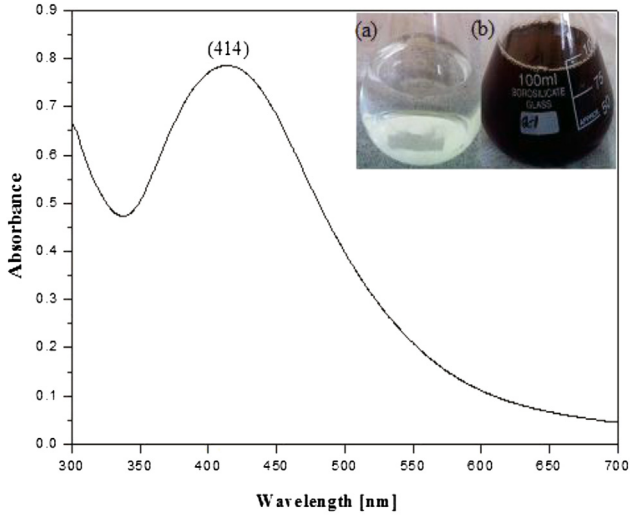

Fig. 1 – UV-vis spectra of phytosynthesized AgNPs. Insert: 1 mM $AgNO_3$ solution (a) without plant extract and (b) with plant extract.

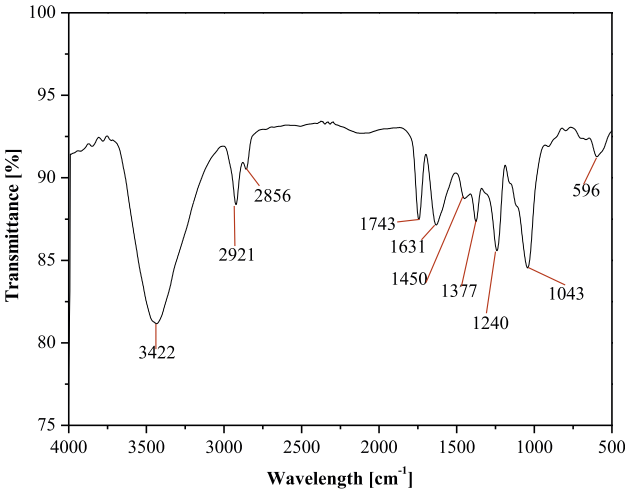

Fig. 2 – FTIR spectra of phytosynthesized AgNPs.

it indicated the formation of AgNPs, while no color change was observed in the absence of plant extract (Fig. 1 insert). In the UV-Vis spectrum; a single, strong and broad Surface plasmon resonance (SPR) peak was observed at 414 nm that confirmed the synthesis of AgNPs. Past studies suggested that a SPR peak located between 410 and 450 nm has been observed for AgNPs and might be attributed to spherical nanoparticles (Zaheer, 2012).

3.3. *Fourier transforms infrared (FTIR) spectroscopy*

FTIR measurements were carried out in order to identify the presence of various functional groups in biomolecules responsible for the bioreduction of Ag^+ and capping/stabilization of silver nanoparticles. The observed intense bands were compared with standard values to identify the functional groups. FTIR spectrum shows absorption bands at 3422, 2921, 2856, 1743, 1631, 1450, 1377, 1240, 1043 and 596 cm^{-1} indicating the presence of capping agent with the nanoparticles (Fig. 2).

The bands at 3422 cm^{-1} in the spectra corresponds to O–H stretching vibration indicating the presence of alcohol and phenol. Bands at 2921 and 2856 cm^{-1} region arising from C–H stretching of aromatic compound were observed. The band at 1743 cm^{-1} was assigned for C–C stretching (non-conjugated). The band at 1631 cm^{-1} in the spectra corresponds to C–N and C–C stretching indicating the presence of proteins (Prakash et al., 2013). The band at 1450 cm^{-1} was assigned for N–H stretch vibration present in the amide linkages of the proteins. These functional groups have role in stability/capping of AgNP as reported in many studies (Niraimathi, Sudha, Lavanya, & Brindha, 2013; Prakash et al., 2013). The bands at 1450 cm^{-1} and 1043 cm^{-1} were assigned for N–H and C–N (amines) stretch vibration of the proteins respectively. The band at 1377 cm^{-1} exemplifies the N=O symmetry stretching typical of the nitro compound. The band at 1240 cm^{-1} corresponds to C–N stretching of amines. The band at 596 cm^{-1} region could be attributed to C–Br stretching, which is characteristic of alkyl halides. It may be concluded from the FTIR spectroscopic study that the secondary structure of proteins in the *U. dioica* Linn. are not affected because of their interaction with Ag^+ ions or nanoparticles.

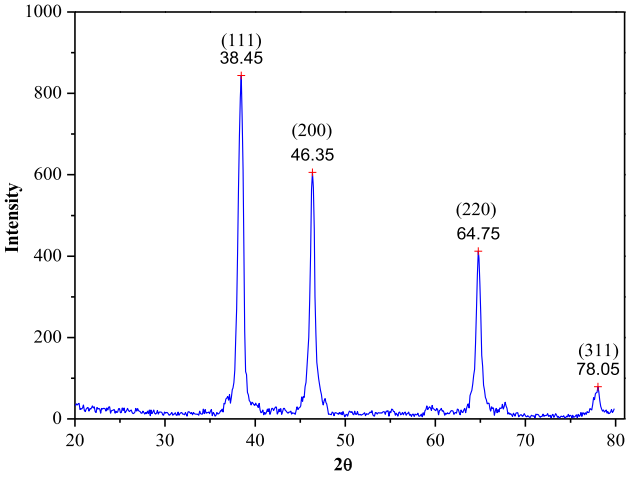

Fig. 3 – XRD analysis of phytosynthesized AgNPs.

3.4. *X-ray diffraction (XRD)*

The crystalline nature of nanoparticles was confirmed by X-ray crystallography. The XRD pattern of the synthesized AgNPs is shown in Fig. 3.

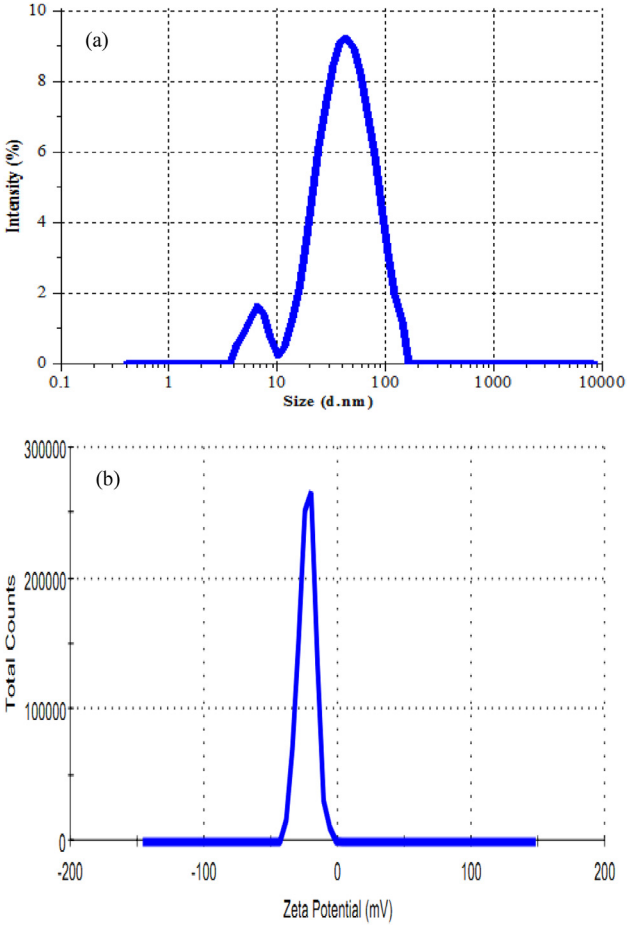

Fig. 4 – (a) Zeta sizer and (b) Zeta potential of phytosynthesized AgNPs.

The diffracted intensities were recorded from 20° to 80°. Four strong Bragg reflections at 38.45°, 46.35°, 64.75° and 78.05° corresponds to the planes of (1 1 1), (2 0 0), (2 2 0) and (3 1 1) respectively which can be indexed according to the facets of face centered cubic crystal structure of silver (Prakash et al., 2013). The interplanar spacing ($d_{calculated}$) values are 2.336, 1.955, 1.436 and 1.224 Å for (1 1 1), (2 0 0), (2 2 0) and (3 1 1) planes respectively and matched with standard silver values [32]. The average crystalline size is calculated using Debye-Scherrer formula,

$$D = \frac{k\lambda}{\beta \cos\theta}$$

Where D is the average crystalline size of the nanoparticles, k is geometric factor (0.9), λ is the wavelength of X-ray radiation source and β is the angular FWHM (full-width at half maximum) of the XRD peak at the diffraction angle θ (Dubey et al., 2010). The calculated average crystallite of the AgNPs is ~25 nm.

3.5. *Particle size distribution and zeta potential measurement*

The size distribution and zeta potential of the AgNPs were determined by DLS (Figs. 4a and b). Particle size distribution curve reveals that AgNPs obtained are polydispersed in nature, with average diameter ~36 nm and the corresponding average zeta potential value is −24.1 mV. The high negative potential value supports long term stability, good colloidal nature and high dispersity of AgNPs due to negative–negative repulsion (Mukherjee et al., 2014).

3.6. *SEM, TEM, EDX and SAED study of AgNPs*

Scanning Electron Microscopy (SEM) and Energy Dispersive X-ray (EDX) studies revealed the spherical nature of particles synthesized from silver metal (Figs. 5a and b).

EDX spectrum reveals strong signal in the silver region and confirms the formation of AgNPs. Metallic silver nanocrystals generally show typical optical absorption peak approximately at 3 KeV due to surface plasmon resonance (Kaviya, Santhanalakshmi, Viswanathan, Muthumar, & Srinivasan, 2011). Silver (70.22%) was the major constituent element compared to copper (28.80%) and oxygen (0.89%) as shown in (Fig. 5b). EDX profile showed strong signal for silver along with weak oxygen peak which may have originated from the biomolecules that are bound to the surface of AgNPs, indicating the reduction of silver ions to elemental silver. Other peak corresponding to Cu in the EDX is an artifact of the Cu-grid on which the sample was coated. There were no peaks observed for silver compounds. This confirms the complete reduction of silver compounds to AgNPs as shown in the spectrum. The Transmission electron microscopy (TEM) provided further insight into the morphology and size details of the synthesized AgNPs. The TEM images at different magnifications and Selected area electron diffraction (SAED) patterns are depicted in the (Figs. 5c and d). The spherical nature of the AgNPs was also witnessed by the TEM with average diameter ranging 20–30 nm. The results ascribed from the XRD pattern are in good agreement with SAED pattern which suggests the polycrystalline nature of AgNPs (Fig. 5e).

3.7. *Antibacterial activity of AgNPs*

The antibacterial activities of phytosynthesized AgNPs were investigated against a range of pathogenic microorganisms using agar disk diffusion method. The diameter of inhibition zone in millimetre is shown in (Table 2) and (Fig. 6). The AgNPs exhibited more activity than $AgNO_3$ solution and leaves extract (taken as controls). Antibacterial activities were found to be increased with the increasing concentration of AgNPs. In present study, zone of inhibition was found to be highest (27 mm) against *S. marcescens* and lowest (18 mm) against *K. pneumoniae*. These findings are in agreement with previous studies that examined antibacterial activity of AgNPs (Ghosh et al., 2012).

The mechanism of the inhibitory action of the metal nanoparticles on microorganisms is not still clearly known. A

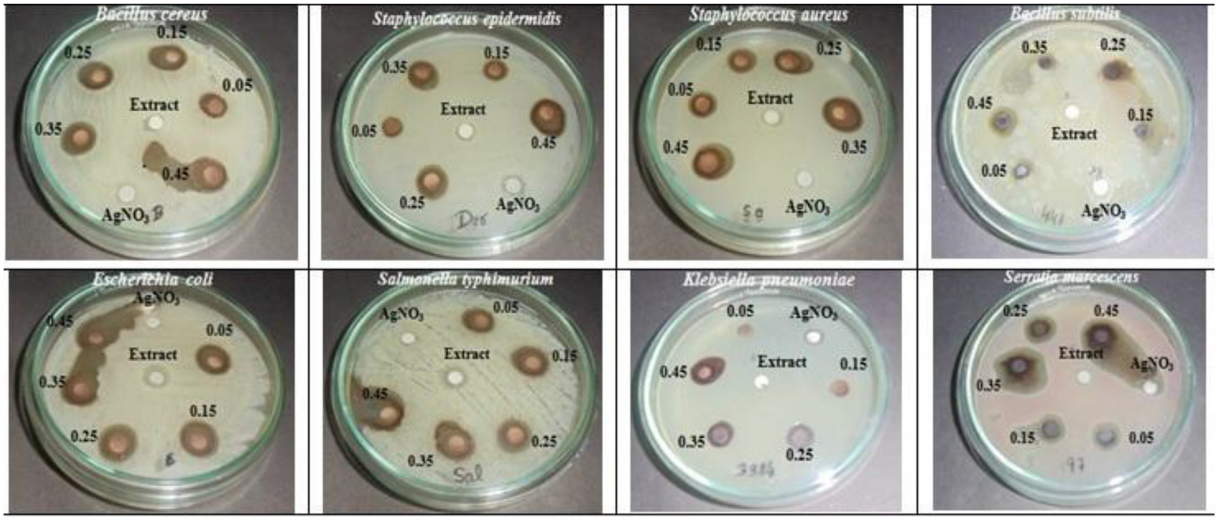

Fig. 5 – Images of antibacterial activities of synthesized silver nanoaprticles of *Urtica dioica*.

Table 2 – Inhibition zone of AgNPs, $AgNO_3$ and *Urtica dioica* Linn. leaves extract against Gram-positive and Gram-negative bacteria.

Test pathogens	Inhibition zone (mm)					Extract	$AgNO_3$
	0.05mg/100 µl	0.15mg/100 µl	0.25mg/100 µl	0.35mg/100 µl	0.45mg/100 µl	0.45mg/100 µl	0.45mg/100 µl
B. cereus	14	15	18	23	24	–	7
S. epidermidis	9	12	14	16	19	7	8
S. aureus	12	16	17	19	21	7	7
B. subtilis	10	12	16	16	25	–	–
E. coli	12	15	16	17	19	9	–
S. typhimurium	14	17	18	19	25	8	7
K. pneumoniae	8	10	13	14	18	–	8
S. marcescens	13	15	16	24	27	7	–

hypothetical mechanism is proposed for antibacterial activities of phytosynthesized AgNPs (Fig 7). The antibacterial effect could be explained on the basis of small sized AgNPs synthesized by *U. dioica* Linn. leaves extract with extremely large surface area that provides better contact and interaction with the bacterial cell than larger ones (Kvitek et al., 2008). This explanation was supported by the TEM results obtained in this work. In addition, silver ions released from AgNPs may penetrate inside the cell membranes interacting with sulfur and phosphorus containing compounds such as proteins and

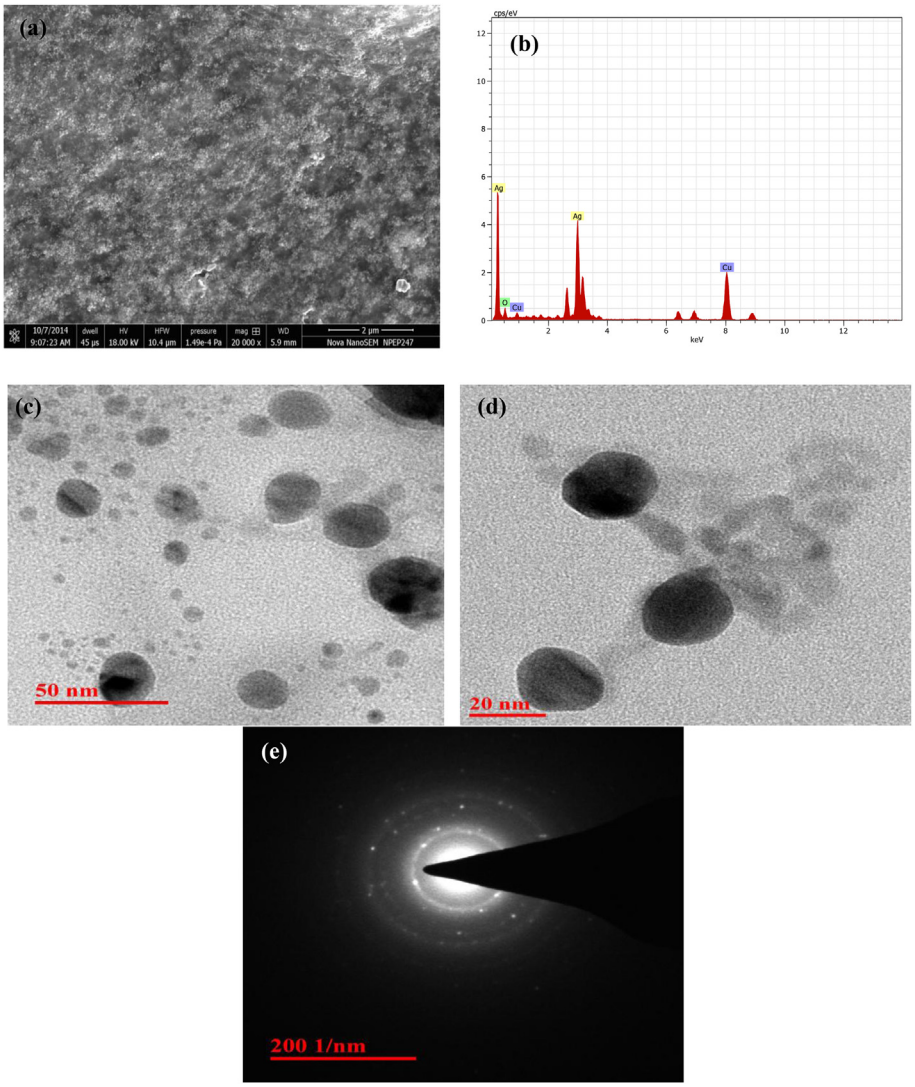

Fig. 6 – (a) SEM observation of phytosynthesized AgNPs (b) Energy dispersive X-ray (EDX) spectrum showed higher percentage of silver signals (c) TEM image of AgNPs at 50 nm range (d) 20 nm range and (e) SAED patterns of the AgNPs exhibit concentric rings, indicating that these nanoparticles are highly crystalline in nature.

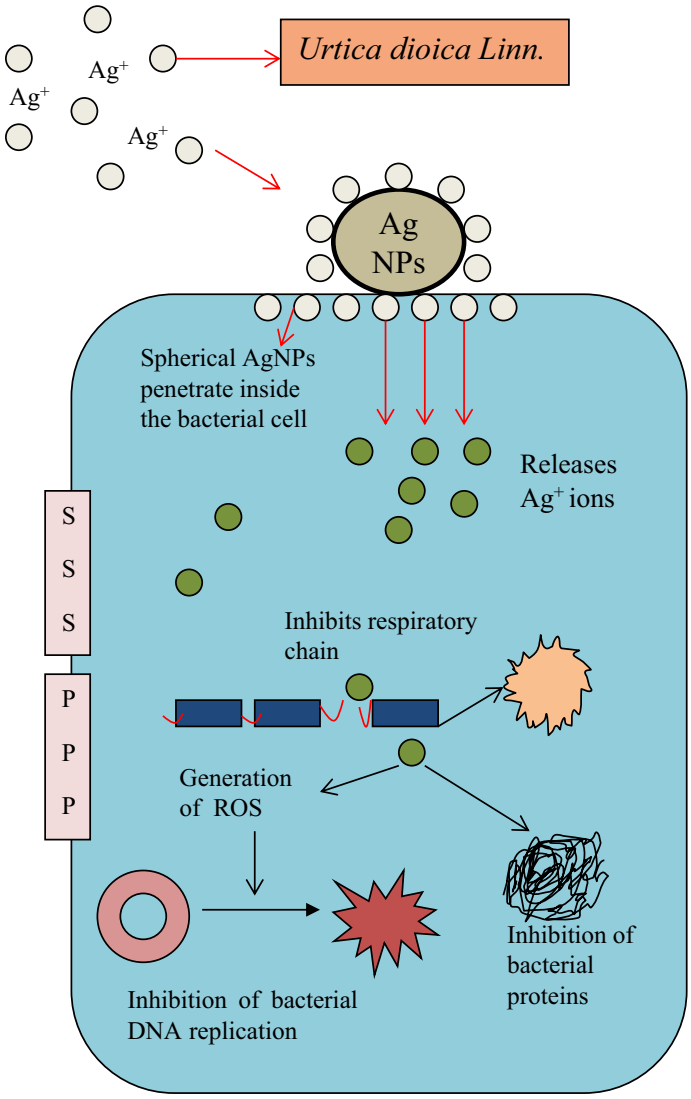

Fig. 7 – Proposed mechanisms of antibacterial activities exerted by *Urtica dioica* Linn. capped AgNPs.

DNA that may inhibit DNA replication and results in loss of cell viability and ultimately leads to cell death (Matsumura, Yoshikata, Kunisaki, & Tsuchido, 2003). It has also been proposed that the AgNPs can have a sustained release of silver ions once inside the bacterial cells (Feng et al., 2001), and these ions can interact with thiol groups present in enzymes such as NADH dehydrogenases and disrupt the respiratory chain (Matsumura et al., 2003). The formation of free radicals by AgNPs induces oxidative stress which may be considered to be another mechanism of cell death (Kim et al., 2007).

3.8. *Synergistic effect of AgNPs with antibiotics*

The synergistic effects of AgNPs with eight antibiotics were investigated against pathogenic bacteria by using agar disk diffusion method in (Table 3) and (Fig. 8). It was observed that effects of antibiotics have increased in most of the cases. Synergistic interaction of AgNPs and streptomycin showed a minute increase in the inhibition zone against seven pathogenic bacteria in the range 0.1–0.9 with the exception of *B. cereus* where a 6.1 fold increase was seen. When combined with Amikacin, Kanamycin, Tetracycline and Cefetaxime, the AgNPs showed comparable synergy (a 0.1–4.4 fold increase). Amoxicillin was found to have the highest overall synergistic activity as observed for *S. marcescens*, a 17.8 fold increase in inhibition zone was seen with the combination of amoxicillin and AgNPs.

For Ampicillin in the presence of AgNPs, a 15.0 fold increase in inhibition zone was observed against *S. marcescens*. The synergistic activity of Vancomycin with AgNPs was observed against *E. coli* (a 10.1 fold increase). A 6.1 fold increase in inhibition zone was found against *S. epidermidis*, *B. subtilis* and *E. coli* in the presence of a combination of Cefepime and AgNPs. *S. epidermidis*, *S. marcescens*, *E. coli*, *S. typhimurium*, *Klebsiella pneumonia*, *S. marcescens* and *B. subtilis* were found to be inhibited in the presence of a combination of

Table 3 – Inhibition zone (mm) of different antibiotics (with and without AgNPs) against gram positive and gram negative bacteria.

Pathogens		Antibiotics								
		Streptomycin	Amikacin	Kanamycin	Vancomycin	Tetracycline	Ampicillin	Cefepime	Amoxicillin	Cefetaxime
B. cereus	A	09	24	15	19	21	25	22	11	33
	B	24	27	25	26	37	28	30	19	39
	C	6.1	0.3	1.7	0.9	2.1	0.2	0.8	1.9	0.4
S. epidermidis	A	27	26	25	18	22	07	06	06	25
	B	35	31	27	18	30	19	16	16	25
	C	0.7	0.4	0.2	0.0	0.8	6.4	6.1	6.1	0.0
S. aureus	A	27	29	26	13	36	29	1 9	15	24
	B	29	32	29	19	39	29	23	20	28
	C	0.1	0.2	0.2	1.1	0.1	0.0	0.5	0.5	0.4
B. subtilis	A	19	23	19	15	12	06	06	06	06
	B	26	26	23	21	19	13	16	13	14
	C	0.9	0.3	0.5	0.9	1.5	3.7	6.1	3.7	4.4
E. coli	A	23	22	15	06	17	06	06	06	06
	B	27	27	15	20	20	14	13	16	13
	C	0.4	0.5	0.0	10.1	0.4	4.4	3.7	6.1	3.7
S. typhimurium	A	22	24	19	12	28	06	06	06	10
	B	31	32	25	20	31	15	14	14	19
	C	0.9	0.8	0.7	1.8	0.2	5.2	4.4	4.4	2.6
K. pneumoniae	A	18	19	20	06	21	11	23	06	25
	B	21	21	22	12	25	16	28	14	30
	C	0.4	0.2	0.2	0.3	0.4	1.1	0.5	4.4	0.4
S. marcescens	A	22	26	24	11	20	06	27	06	16
	B	27	26	26	11	27	24	27	26	20
	C	0.5	0.0	0.2	0.0	0.8	15.0	0.0	17.8	0.6

Note: All experiments were performed in triplicates and standard deviations were negligible. Increase in fold area of individual antibiotics were calculated as $C = B^2 - A^2/A^2$, where, A and B are the inhibition zones (mm) obtained for antibiotic alone and antibiotics + AgNPs, respectively. In case of no zone of inhibition, diameter of the disk (6 mm) was taken for the calculation.

AgNPs and antibiotics, which otherwise showed a resistant pattern in the presence of the antibiotics (Vancomycin, Cefetaxime, Ampicillin, Kanamycin, Amikacin, Cefepime) alone. It is concluded that AgNPs have augmented the efficacy of most of the antibiotics, therefore, may be used in combination with antibiotics against drug resistant bacteria. Our results are also in correlation with the work previously done by some researchers studied the synergistic effect of silver nanoparticles alone and in combination with conventional antibiotics against pathogenic strains (Fayaz et al., 2010; Ghosh et al., 2012; Singh et al., 2013). Moreover, this research provides helpful insight into the development of new antibacterial agents. The combination of antibiotics and AgNPs will make it difficult for pathogenic bacteria to develop resistance which otherwise renders the available antibiotics inefficient, hence, this combination therapy can be further studied to develop new formulation of AgNPs in synergy with antibiotics.

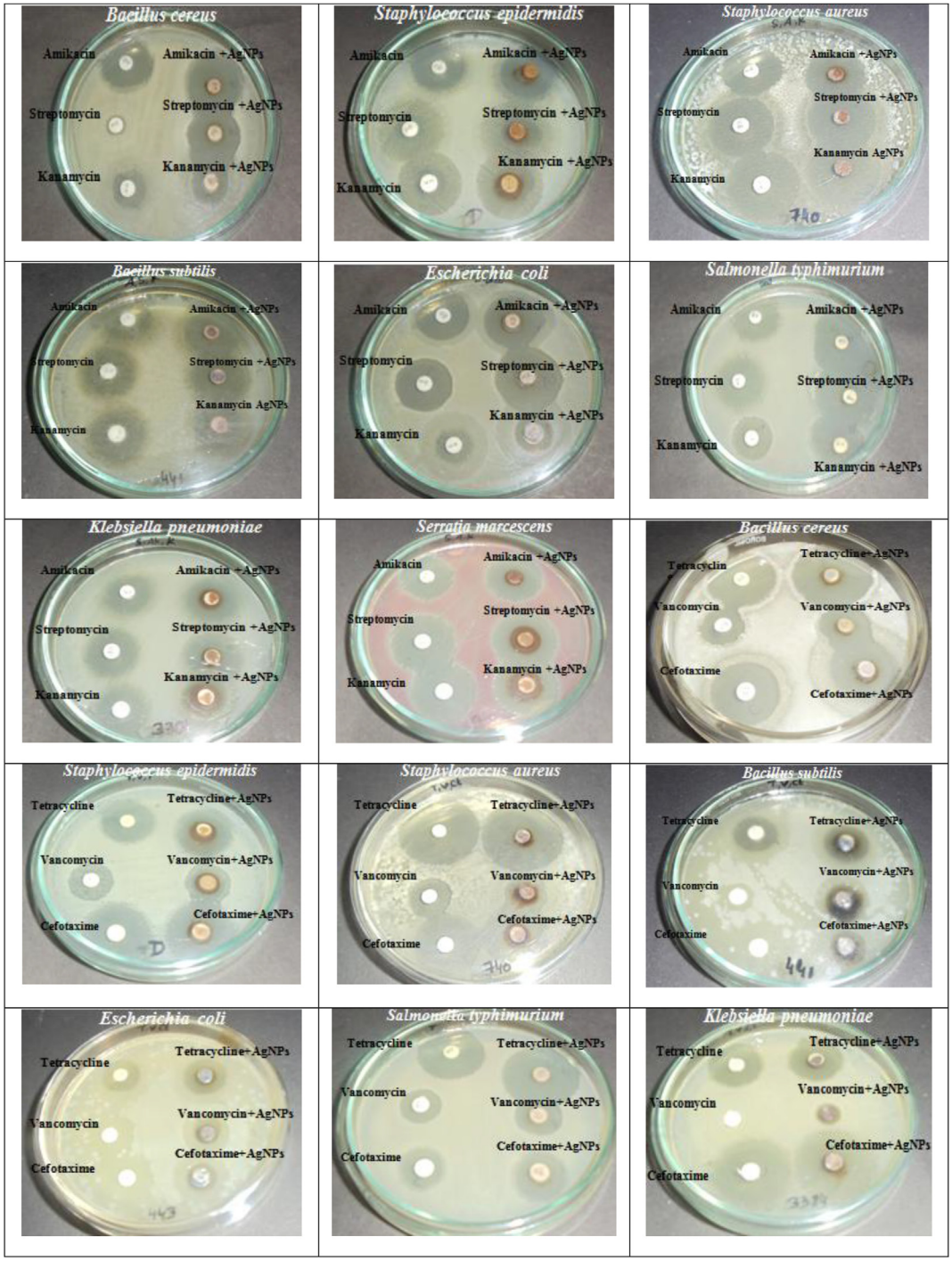

Fig. 8 – Plates showing the increase in diameter of inhibition zone of antibiotics with AgNPs against pathogenic bacteria.

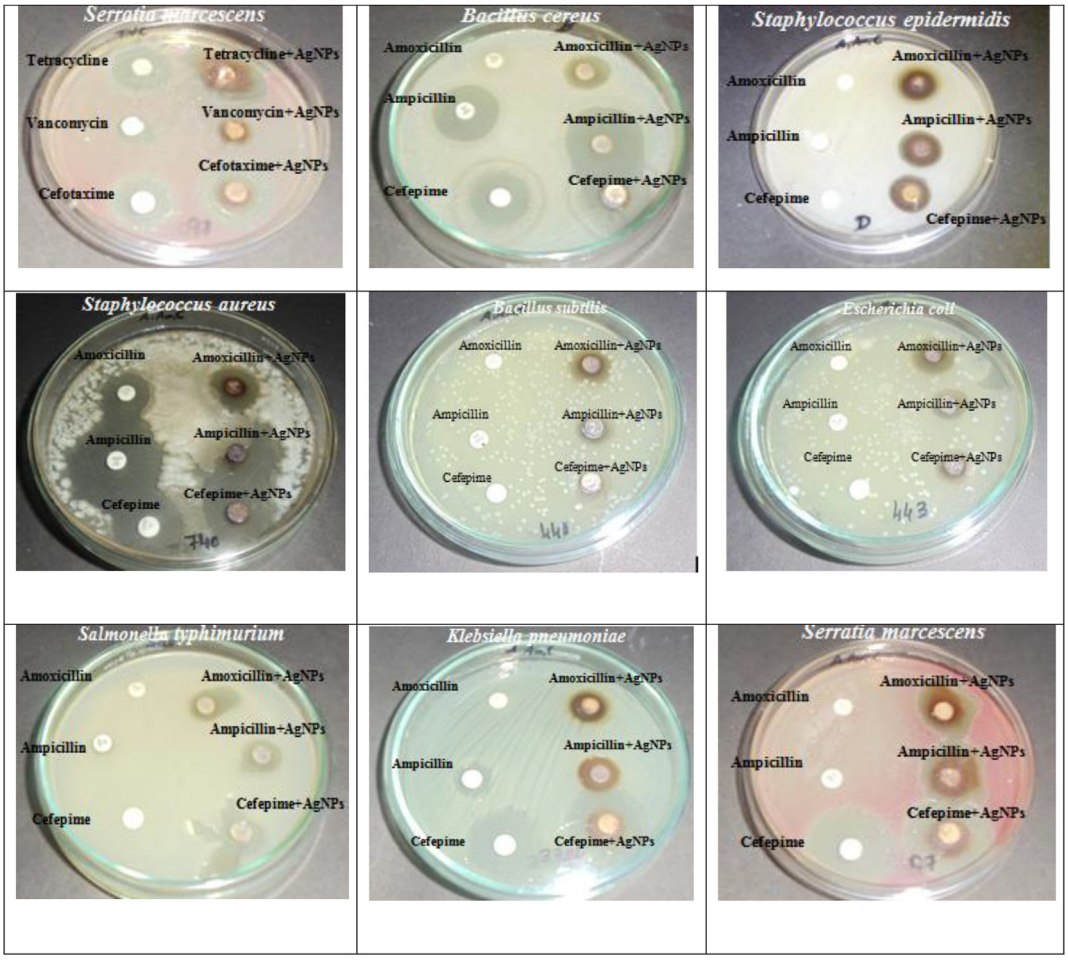

Fig. 8 – (*continued*).

4. Conclusions

In the present investigation, novel approach for biosynthesis of AgNPs from leaves extract of *U. dioica* Linn. was given. The synthesized AgNPs were spherical in shape with size ranging around 20–30 nm as observed in SEM/TEM and XRD analysis. The synthesized AgNPs have shown antibacterial and synergistic activity with conventional antibiotics against a wide range of pathogenic bacteria which established their application in biomedicines. Thus, it is concluded that the phytosynthesis of AgNPs using *U. dioica* leaves extract is a cost effective, simple and ecofriendly method that excludes the hazards arising out of the use of harmful reducing/capping agents. Moreover, this process could be easily scaled up for the industrial applications to increase the yield of the nanopartilces significantly, which undoubtedly would establish its commercial viability in medicine.

Acknowledgments

This study was conducted in the Department of Biotechnology, G.B. Pant Engineering College (GBPEC), Pauri Garhwal (Uttarakhand). Authors gratefully acknowledge the necessary instrumental facilities, consumables and constant supervision provided by the Department of Biotechnology, Govind Ballabh Pant Engineering College, Pauri Garhwal, Uttarakhand, India.

REFERENCES

Ashokkumar, S., Ravi, S., Kathiravan, V., & Velmurugan, S. (2014). Synthesis, characterization and catalytic activity of silver nanoparticles using *Tribulus terrestris* leaf extract. *Spectrochimica Acta Part A: Molecular and Biomolecular Spectroscopy*, 121, 88–93.

Chandran, S. P., Chaudhary, M., Pasricha, R., Ahmed, A., & Sastry, M. (2006). Synthesis of gold nanotriangles and silver nanoparticles using *Aloe vera* plant extract. *Biotechnology Progress*, 22, 577–583.

Cormican, M. G., Wilke, W. W., Barrett, M. S., Pfaller, M. A., & Jones, R. N. (1996). Phenotypic detection of mec A-positive staphylococcal blood stream isolates: high accuracy of simple disk diffusion tests. *Diagnostic Microbiology Infection Disease*, 25, 107–112.

Dubey, S. P., Lahtinen, M., & Sillanpaa, M. (2010). Tansy fruit mediated greener synthesis of silver and gold nanoparticles. *Process Biochemistry*, 45, 1065–1071.

Duran, N., Marcarto, P. D., DeSouza, G. I. H., Alves, O. L., & Esposito, E. (2007). Antibacterial effect of silver nanoparticles produced by fungal process on textile fabrics and their effluent treatment. *Journal of biomedical nanotechnology, 3*, 203–208.

Edgar, S., Sofia, S., Sonia, M., & Correia, J. (2014). PVP coated silver nanoparticles showing antifungal improved activity against Dermatophytes. *Journal of nanoparticles research, 16*, 2726.

Fayaz, A. M., Balaji, K., Girilal, M., Yadav, R., Kalaichelvan, P. T., & Venketesan, R. (2010). Biogenic synthesis of silver nanoparticles and their synergistic effect with antibiotics: a study against gram-positive and gram-negative bacteria. *Nanomedicine: Nanotechnology, Biology and medicine, 6*, 103–109.

Feng, Q. L., Wu, J., Chen, G. Q., Cui, F. Z., Kim, T. N., & Kim, J. O. (2001). A mechanistic study of the antibacterial effect of silver ions on *Escherichia coli* and *Staphylococcus aureus*. *Journal of Biomedical Materials Research, 52*, 662–668.

Fransworth, N. R. (1996). Biological and phytochemical screening of plants. *Journal of Pharmaceutical Sciences, 55*, 225–227.

Ghosh, S., Patil, S., Ahire, M., Kitture, R., Kale, S., Pardesi, K., et al. (2012). Synthesis of silver nanoparticles using *Dioscorea bulbifera* tuber extract and evaluation of its synergistic potential in combination with antimicrobial agents. *International journal of Nanomedicine, 7*, 483–496.

Gulcin, I., Kufrevioglu, O. I., Oktay, M., & Buyukokuroglu, M. E. (2004). Antioxidant, antimicrobial, antiulcer and analgesic activities of nettle (*Urtica dioica*). *Journal of Ethnopharmacology, 90*, 205–215.

Jacob, J. A., Biswas, N., Mukherjee, T., & Kapoor, S. (2011). Effect of Plant-based phenol derivatives on the formation of Cu and Ag nanoparticles. *Colloids and Surfaces B: Biointerfaces, 87*, 49–53.

Jeyaraj, M., Sathishkumar, G., Sivanandhan, G., Ali, D. M., Rajesh, M., Arun, R., et al. (2013). Biogenic silver nanoparticles for cancer treatment: an experimental report. *Colloids and Surfaces B: Biointerfaces, 106*, 86–92.

Jha, A. K., Prasad, K., Prasad, K., & Kulkarni, A. R. (2009). Plant system: nature's nanofactory. *Colloids and Surfaces B: Biointerfaces, 73*, 219–223.

Kasthuri, J., Kathiravan, K., & Rajendiran, N. (2009). Phyllanthin-assisted biosynthesis of silver and gold nanoparticles: a novel biological approach. *Journal of Nanoparticles Research, 11*, 1075–1085.

Kaviya, S., Santhanalakshmi, J., Viswanathan, B., Muthumar, J., & Srinivasan, K. (2011). Biosynthesis of silver nanoparticles using citrus sinensis peel extract and its antibacterial activity. *Spectrochimica Acta Part A: Molecular and Biomolecular Spectroscopy, 79*, 594–598.

Kim, J. S., Kuk, E., Yu, K., Kim, J. H., Park, S. J., Lee, H. J., et al. (2007). Antimicrobial effects of silver nanoparticles. *Nanomedicine, 3*, 95–101.

Kowshik, M., Ashtaputre, S., Kharrazi, S., Vogel, W., Urban, J., Kulkarni, S. K., et al. (2003). Extracellular synthesis of silver nanoparticles by a silver-tolerant yeast strain MKY3. *Nanotechnology, 14*, 95.

Kumar, P., Govindaraju, M., Senthamilselvi, S., & Premkumar, K. (2013). Photocatalytic degradation of methyl orange dye using silver (Ag) nanoparticles synthesized from *Ulva lactuca*. *Colloids and Surfaces B: Biointerfaces, 103*, 658–661.

Kvitek, L., Panacek, A., Soukupova, J., Kolar, M., Vecerova, R., Prucek, R., et al. (2008). Effect of surfactants and polymers on stability and antibacterial activity of silver nanoparticles (NPs). *Journal of Physical Chemistry C, 112*, 5825–5834.

Mallick, K., Witcomb, M. J., & Scurell, M. S. (2004). Polymer stabilized silver nanoparticles: a photochemical synthesis route. *Journal of Material Science, 39*, 4459–4463.

Matsumura, Y., Yoshikata, K., Kunisaki, S., & Tsuchido, T. (2003). Mode of bactericidal action of silver zeolite and its comparison with that of silver nitrate. *Applied and Environmental Microbiology, 69*, 4278–4281.

Mukherjee, S., Chowdhury, D., Kotcherlakota, R., Patra, S., Vinothkumar, B., Bhadra, M. P., et al. (2014). Potential theranostics application of bio-synthesized silver nanoparticles (4-in-1 system). *Theranostics, 4*, 316–335.

Namasivayam, S. K. R., Gnanendra, K. E., & Reepika, R. (2010). Synthesis of silver nanoparticles by *Lactobacillus acidophilus* 01 strain and evaluation of its in vitro genomic DNA toxicity. *Nano-Micro Letters, 2*, 160–163.

Niraimathi, K. L., Sudha, V., Lavanya, R., & Brindha, P. (2013). Biosynthesis of silver nanoparticles using Alternanthera sessilis (Linn.) extract and their antimicrobial, antioxidant activities. *Colloids and Surfaces B: Biointerfaces, 102*, 288–291.

Prakash, P., Gnanaprakasam, P., Emmanuel, R., Arokiyaraj, S., & Saravanan, M. (2013). Green synthesis of silver nanoparticles from leaf extract of *Mimusops elengi*, Linn. for enhanced antibacterial activity against multi drug resistant clinical isolates. *Colloids and Surfaces B: Biointerfaces, 108*, 255–259.

Raghunandan, D., Bedre, M. D., Basavaraja, S., Sawle, B., Manjunath, S., & Venkataraman, A. (2010). Rapid synthesis of irregular shaped gold nanoparticles from macerated aqueous extracellular dried clove buds (*Syzygium aromaticum*) solution. *Colloids and Surfaces B: Biointerfaces, 79*, 235–240.

Rati, R. N., Nilotpala, P., Debadhyan, B., Kshyama, M. P., Srabani, M., Lala, B. S., et al. (2011). Green synthesis of silver nanoparticle by Penicillium purpurogenum NPMF: the process and optimization. *Journal of Nanoparticles Research, 13*, 3129–3137.

Saravanan, M., Vemu, A. K., & Barik, S. K. (2011). Rapid biosynthesis of silver nanoparticles from *Bacillus megaterium* (NCIM 2326) and their antibacterial activity on multi drug resistant clinical pathogens. *Colloids and Surfaces B: Biointerfaces, 88*, 325–331.

Sheny, D. S., Philip, D., & Mathew, J. (2012). Rapid green synthesis of palladium nanoparticles using the dried leaf of *Anacardium occidentale*. *Spectrochimica Acta Part A: Molecular and Biomolecular Spectroscopy, 91*, 35–38.

Singh, R., Wagh, P., Wadhwani, S., Gaidhaini, S., Kumbhar, A., Bellare, J., et al. (2013). Synthesis, optimization, and characterization of silver nanoparticles from *Acinetobacter calcoaceticus* and their enhanced antibacterial activity when combined with antibiotics. *International Journal of Nanomedicine, 8*, 4277–4290.

Sunita, R. B., Veera, R. G., Tushar, K. G., Robert, V. T., & Sudarshan, K. L. (2011). Gold, silver, and palladium nanoparticle/nano-agglomerate generation, collection, and characterization. *Journal of Nanoparticles Research, 13*, 6591–6601.

Thakkar, K. N., Mhatre, S. S., & Parikh, R. Y. (2010). Biological synthesis of metallic nanoparticles. *Nanomedicine, 6*, 257–262.

Tiwari, D. K., Behari, J., & Sen, P. (2008). Time and dose-dependent antimicrobial potential of Ag nanoparticles synthesized by top-down approach. *Current science, 95*, 647–655.

Torres, S. K., Campos, V. L., León, C. G., Rodríguez-Llamazares, S. M., Rojas, S. M., González, M., et al. (2012). Biosynthesis of selenium nanoparticles by *Pantoea agglomerans* and their antioxidant activity. *Journal of Nanoparticles Research, 14*, 1236.

Vlerken, L. E. V., & Amiji, M. M. (2006). Multi-functional polymeric nanoparticles for tumor- targeted drug delivery. *Expert opinion on Drug Delivery, 3*, 205–216.

Zaheer, Z., & Rafiuddin. (2012). Silver nanoparticles to self-assembled films: green synthesis and characterization. *Colloids and Surfaces B: Biointerfaces, 90*, 48–52.